

Structural, Electrical and Magnetic Properties of NCCF+ BTO ME Composites

P. B. Belavi, L. R. Naik, R. K. Kotnala, V. L. Mathe

Abstract— The magnetoelectric (ME) composites with the composition $(y) \text{Ni}_{0.75}\text{Cd}_{0.2}\text{Cu}_{0.05}\text{Fe}_2\text{O}_4$ (NCCF)+ $(1-y) \text{BaTiO}_3$ (BTO), in which $0 \leq y \leq 1$, were synthesized by standard double sintering ceramic method. The characteristic structural properties of the composites were studied by various techniques such as XRD, SEM and EDX. The XRD patterns of the composites revealed cubic spinel structure of ferrite and tetragonal perovskite structure of ferroelectrics. The microstructural aspects of the composites observed by using SEM; revealed the effect of constituent phases on the average grain size of composites. The elemental identification of the composites studied by using EDX technique are in good agreement with the expected values and shows the absence of impurities present in the composites. The temperature dependent dc resistivity of the composites shows the semiconducting nature of the sample. The dielectric constant and dielectric loss tangent was measured as a function of frequency [20 Hz to 1 MHz]. In the low frequency region [20 Hz to 1 kHz] usual dielectric dispersion behavior was observed, it was due to Maxwell-Wagner type of interfacial polarization. The linear variation in ac conductivity with frequency shows small polaron hopping type of conduction mechanism in the composites. Magnetization measurement of the composites carried out by using VSM at room temperature reveals soft magnetic behavior and showed linear effect on the saturation magnetization and magnetic moment of the composites with ferrite content. The saturation polarization and remnant polarizations decreases with increasing frequency as well as ferrite content in the composites. Further the multiferroic behavior was confirmed by their ME response at room temperature. Maximum ME voltage coefficient (15.6 mV/cmOe) was found in composite sample containing 15 mole % of ferrite and 85 mole % ferroelectric phases and is due to high resistivity and small average grain size of the sample compared to other composite samples.

Index Terms— Sintering, microstructure, SEM, EDX, dc resistivity, dielectric properties, multiferroic properties

1 INTRODUCTION

Structural, electrical, dielectric and magnetic properties of multiferroic ME composites have led to an increased interest among the researchers due to their wide applications in various fields. The possibility of developing smarter and smaller multifunctional devices is a fashion and interest of many researchers. Infact, ME composites the combinations of ferrites and ferroelectrics have found wide applications in electronic devices where higher densities, limited space and multifunctions are required. At the same time significant efforts are being made to understand the science of multiferroic and magnetoelectric behavior in the composites and its application towards the development of high sensitive materials [1-5]. Ferroelectric materials with spontaneous electric polarization that can be switched by an applied electric field are widely used as tunable capacitors and ferroelectric random access memory (Fe-RAM) for computers. On the other hand, ferromagnetic materials with a spontaneous magnetization that can be reversed by a magnetic field are widely used for recording and data storage, such as magnetic random access memory (MRAM) in hard drive.

The ME composite materials show multiferroic properties such as magnetoelectric behavior. The term multiferroic was due to Schmid in 1994, these materials have increased interest because of their potential applications in multi-state memories, spintronics and heterogeneous read/write devices [1-3].

- L R Naik, Professor, Department of Studies in Physics, Karnatak University, Dharwad - 580 003, Karnataka, India
naik_36@rediffmail.com
- P.B. Belavi, Gogte Engineering College, Belgaum, India
- R. K. Kotnala, National Physical Laboratory, New Dehli
- V. L. Mathe, Department of Physics, University of Pune, India

In multiferroic materials, the coupling interaction between different order parameters can induce new effects, such as magnetoelectric, magneto optic and magnetoelastic effect [4, 5]. ME composites exhibits individual properties of ferrites and ferroelectrics and produce a giant magnetoelectric effect due to their product property. Van Suchtelen was first person to propose the concept of magnetoelectric effect in the composites in 1972 at the Philips Laboratory [6]. Later on bi phase ME composites have drawn significant interest in recent years in which the coupling interaction between the ferrite and ferroelectric materials produces a large ME response. The magnetoelectric effect in these materials can be defined as a change of electric polarization upon the application of applied magnetic field $(ME)_H$ or an induced magnetization upon the application of external electric field $(ME)_E$ [7]. However, under the action of alternating magnetic field, the strain induced by magnetostrictive phase was converted into electric charge and is called direct magnetoelectric effect (DME) (eq.1). On the other hand the strain induced by piezoelectric phase under the action of applied electric field was transferred to the magnetostrictive phase and converts into magnetic field called converse magnetoelectric effect (CME) (eq.2). The possibility of conversion of electric energy into magnetic energy and vice-versa are given below

$$DME = \frac{\text{Magnetic}}{\text{Mechanical}} \times \frac{\text{Mechanical}}{\text{Electric}} \quad (1)$$

$$CME = \frac{\text{Electric}}{\text{Mechanical}} \times \frac{\text{Mechanical}}{\text{Magnetic}} \quad (2)$$

Then,

$$ME = \left(\frac{\text{Strain induced}}{\text{Magnetic field}} \right)_{\text{Ferrite}} \times \left(\frac{\text{Electric field}}{\text{Stress induced}} \right)_{\text{Ferroelectric}} \quad (3)$$

These ME composite provides an opportunity for potential applications in multifunctional devices, such as magnetoelectric memory, magnetoelectric sensors, transducers and actuators [8, 9]. However, the proper choice of constituent phases in particulate composites such as ferrite and ferroelectric materials mainly depends on the magnetostriction coefficient, high piezoelectric coupling constant, high dielectric permittivity and high poling strength [10]. The composites containing ferrite phase ($\text{Ni}_{0.75}\text{Cd}_{0.2}\text{Cu}_{0.05}\text{Fe}_2\text{O}_4$) and ferroelectric phase (BaTiO_3) are expected to show good electrical, dielectric and multiferroic properties. Infact Ni-Cd-Cu ferrites have wide microwave applications in electronics, circulators, isolators, phase shifters, ferrite wave absorbers, humidity sensors and thermo junctions, by virtue of their high saturation magnetization, high stability and low dielectric loss at high frequency region [11]. At the same time barium titanate (BaTiO_3) is the most common ferroelectric oxide in the perovskite ABO_3 structure, and it has high dielectric constant, piezoelectric coupling constant and low dielectric loss. Jahn-Teller ions like Ni^{2+} and Cu^{2+} with high coupling coefficient contributes more towards the magnetostriction as the large value of magnetostriction is one of the basic requirement for composites to exhibit large ME effect.

In the present work the standard double sintering ceramic method was used to synthesize ME composites of our interest. In this method microstructural aspects such as grain size, orientation of grains, porosity and sintering temperature can be easily controlled and their effect on ME conversion factor can be studied easily and effectively. Therefore the present work is focused on synthesis, characterization, dc resistivity, dielectric, ferromagnetic, ferroelectric and multiferroic properties of these ME composites. Also we report the effect of composition, grain size as well as resistivity on ME effect in these composites.

2. Experimental details

2.1. Synthesis

The composites consisting of ferrite ($\text{Ni}_{0.75}\text{Cd}_{0.2}\text{Cu}_{0.05}\text{Fe}_2\text{O}_4$) phase and ferroelectric (BaTiO_3) phase were synthesized by using standard double sintering ceramic method. The ferrite phase was synthesized by using AR grade NiO, CdO, CuO and Fe_2O_3 and the ferroelectric phase was synthesized by using AR grade BaCO_3 and TiO_2 powders in stoichiometric proportions. Thereafter they are well grinded for few hours in a planetary agate mortar. Later on ferrite and ferroelectric powders were presintered at 800 °C for 8 hrs in a programmable furnace and slowly cooled to room temperature. The composites were prepared by mixing the presintered 15, 30 and 45 mole % of ferrite phase with 85, 70 and 55 mole % of ferroelectric phase in acetone medium and again milled for few hours in a planetary agate mortar. The well mixed powders were presintered at 800 °C for 8 hrs by slowly increasing temperature at the rate of 100 °C/hrs and cooled to room temperature in a programmable furnace at the same rate. Thereafter 2% of

polyvinyl alcohol was added as a binder to the presintered powder and again grinded and pressed in to pellets of about 10 mm in diameter and 2-3 mm in thickness using a die and hydraulic press by applying a pressure of about 6-7 ton/sq.inch for 5 min. The pellets of composites and constituent phases were finally sintered at 1150 °C for 12 hrs in air medium for the completion of the solid state reaction and then cooled to room temperature at the same rate in the furnace.

2.2. Characterization

The X-ray diffraction pattern of all the synthesized composites were obtained by using Philips Model PW-1710 X-ray diffractometer with Cu-K α radiation ($\lambda = 1.5405 \text{ \AA}$) in the 2θ range from 10° to 80° in a step of 0.04° per second. The formation of bi-phases i.e. cubic spinel structure of ferrite phase and tetragonal perovskite structure of ferroelectric phase in the ME composites were confirmed by X-ray diffraction pattern. The surface morphology and elemental identification of composites were carried out by using scanning electron microscopy (ESEM Quanta 200, FEI) attached with energy dispersive X-ray spectroscopy (EDX). For the measurement of dc resistivity, the final sintered composite samples with well polished and silver paste coated surface were used to get good ohmic contact. The temperature dependent dc resistivities of the composites were carried out by using two probe methods. An impedance analyzer (Model 6540A Wayne Kerr, UK) was used to estimate the parallel capacitance (C_p) and dielectric loss tangent ($\tan\delta$) of the composite pellets (silver pasted) at room temperature in the wide range of frequencies from 20 Hz to 1 MHz then dielectric constant of the composites was calculated using the following relation [10],

$$\epsilon' = \frac{C_p t}{\epsilon_o A} \quad (4)$$

Where C_p is the parallel capacitance, t is the thickness, ϵ_o is the permittivity of free space ($8.854 \times 10^{-14} \text{ F/cm}$), A is the surface area of the pellet. The ac conductivity of the composites at different frequencies was estimated at room temperature using the relation [10],

$$\sigma_{ac} = \epsilon' \epsilon_o \omega \tan \delta \quad (5)$$

The ferroelectric P-E loops of the composite samples were characterized by using Radiant Technologies Ferroelectric Loop Tracer (*Precision Premier II Model*) interfaced with computer and was used to measure the saturation polarization and remnant polarization for two fixed frequencies i.e. 50 and 200 Hz at room temperature.

The ferromagnetic hysteresis loops at room temperature as well as temperature dependence magnetization of the composites were performed using vibrating sample magnetometer (VSM Model 735, Lakeshore). The magnetization per gram (σ_s') of the composite samples was estimated using the relation [10].

$$M_s = (1-p) \sigma_s' d_x \quad (6)$$

Where p is porosity, M_s is the saturation magnetization and d_x is the X-ray density. The magnetic moment of the composites (in Bohr magneton) was calculated using the relation.

$$\mu_B = \frac{M\sigma_s'}{5585} \quad (7)$$

Where, M is the molecular weight of the samples. Static ME voltage coefficient of all the composites were measured as a function of dc magnetic field. In order to estimate the static ME voltage coefficient the proper electric poling was made by heating the samples to about 20 - 30 °C above the ferroelectric Curie temperature (T_c) and then cooled to room temperature under the influence of an external electric field of 2-2.5 kV/cm. These electrically poled samples were magnetically poled by applying a dc magnetic field of about 4.2 kOe at room temperature. For magnetic poling laboratory made sample holder was used. Thereafter the pellet is kept in between two plates i.e. sample holder and then it is connected to the poles of a dc electromagnet. The dc magnetic field was applied in the direction of applied electric field and perpendicular to the polished and flat surfaces of the pellets. The stray charges developed during the poling process were eliminated by grounding the pellet holding plates. The electric field generated across the sample under the influence of dc magnetic field was measured by using Keithley electrometer (model 2000).

3. Results and discussion

3.1. Structural properties

3.1.a. XRD studies

The X-ray diffraction patterns of the composites are shown in figure 1. All the peaks appeared in the diffraction patterns are identified by comparing with JCPD's data. The occurrence of peaks with specific indices confirms the formation cubic spinel structure of ferrite phase and tetragonal perovskite structure of ferroelectric phase within the composites. However, the non-occurrence of additional peaks other than those belonging to cubic spinel structure of ferrite phase and tetragonal perovskite structure of ferroelectric phase suggests the absence of apparent chemical reaction, mutual solubility between the two phases and shows the purity of the samples. The lattice parameter of the constituent phases and their composites are estimated and are found to be nearly equal to their parent phases (table 1). The constant value of tetragonality ratio c/a for the prominent peak (1 1 0) with mol % of ferrite and ferroelectric phases in the composites suggests non variation in its structure. The systematic variation of the diffraction intensities of the ferrite and ferroelectric phases in the composites were observed with the variation of the ferrite content in the composites. With the increase of the ferrite content in the composites the intensity of ferrite peak (3 1 1) increases while the intensity of ferroelectric peak (1 1 0) decreases. The lattice parameter of the ferrite phase estimated was found to increase with mol % of ferrite in the composite, it was due to the difference in the ionic radii of component ions as Cd²⁺ ion have larger ionic radii (0.097nm) than Cu²⁺ (0.073nm), Ni²⁺ (0.069nm) and Fe³⁺ (0.0644nm) ions [10].

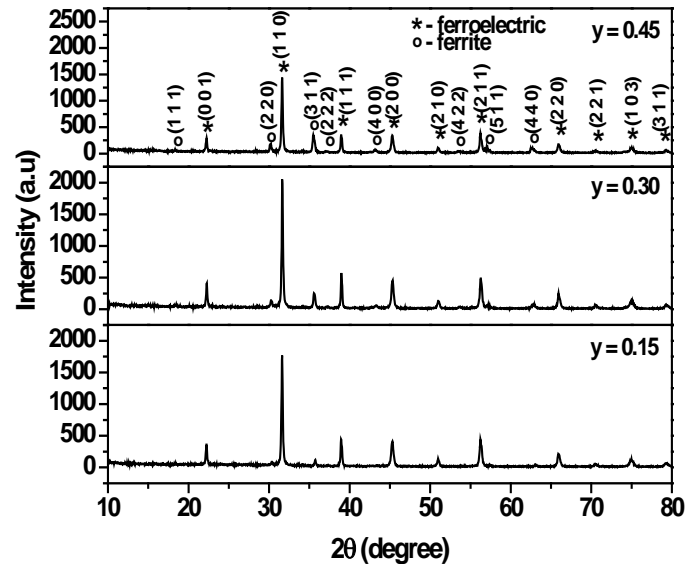


Fig 1. XRD patterns of (y) Ni_{0.75}Cd_{0.2}Cu_{0.05}Fe₂O₄ + (1-y) BaTiO₃ ME composites

3.1.b. SEM studies

The SEM micrographs of the composites as a function of ferrite content are shown in figure 2 (a - c). In these figures the fine particles with highly dense microstructure and proper grain growth without segregation of impurity were seen. The average grain sizes of the composite were estimated from SEM micrographs using Cottrell's method [11] and are tabulated in table 1. The absence of third phase in XRD patterns and SEM micrographs of composites suggests the probability of inter diffusion between two phases during the final stage of the sintering is negligible. The average grain size of pure ferrite phase is more compared to pure ferroelectric phase in the composites. The average grain size of the composites was found to increase where as the porosity was found to decrease with increasing the ferrite content, it may be due to the difference in grain sizes of the constituent phases, and is one of the key factors for getting the high ME output in these composites. As the grain size increases the grain boundary area and porosity decreases (table 1), which acts as an obstacle for domain wall motion and this affects to dc resistivity, dielectric, magnetic and magnetoelectric properties of ME composites. The increase of average grain size with ferrite content in the composites results in an increase of mean free path of electron and dielectric constant. The presence of pores in the composites breaks the magnetic circuit between the grains. In the present composites as the ferrite content increases the porosity of the composite decreases and supports the increase of net magnetization. The magnetization of the composites increases more easily with increased average grain size as well as ferrite content. The large average grain sizes are less effective in inducing piezomagnetic and piezoelectric coefficient rather than the smaller ones [12]. In the present work small average grain size with minimum porosity and uniform distribution of ferrite

particles into ferroelectric matrix in the composites were observed and these parameters supports for getting the high ME effect in these composites.

3.1.c. EDX studies

The elemental identification of the composites was done with EDX technique. The EDX spectra of the composites are shown in figure 3(a-c).

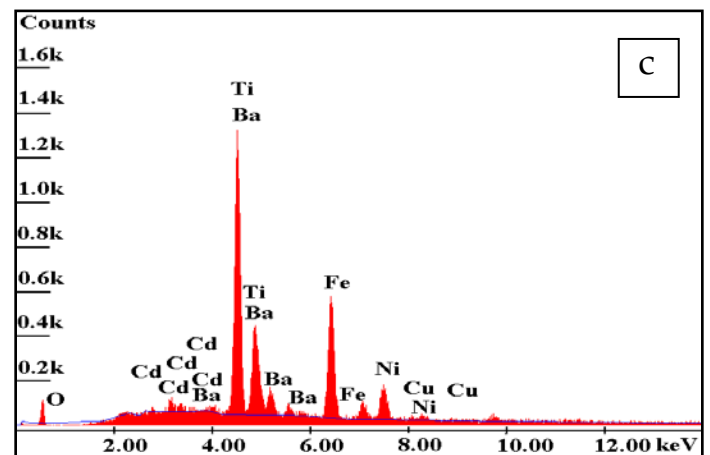
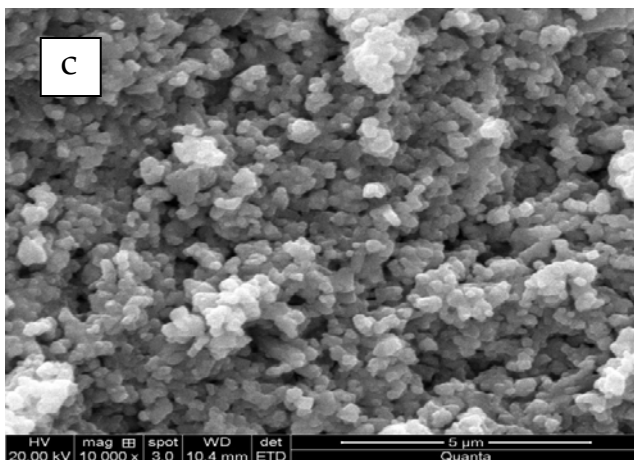
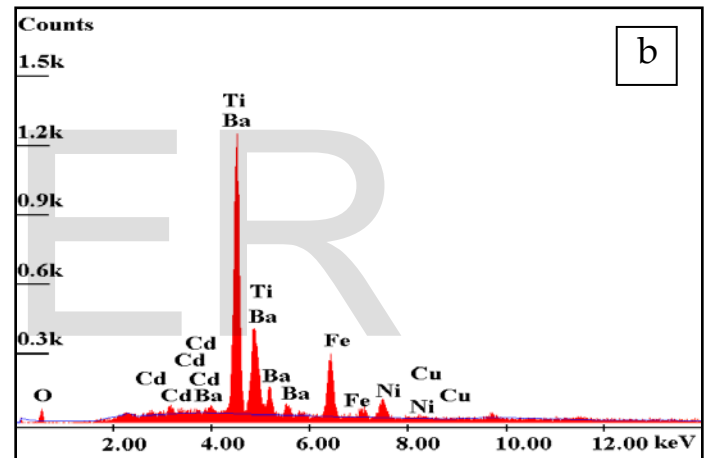
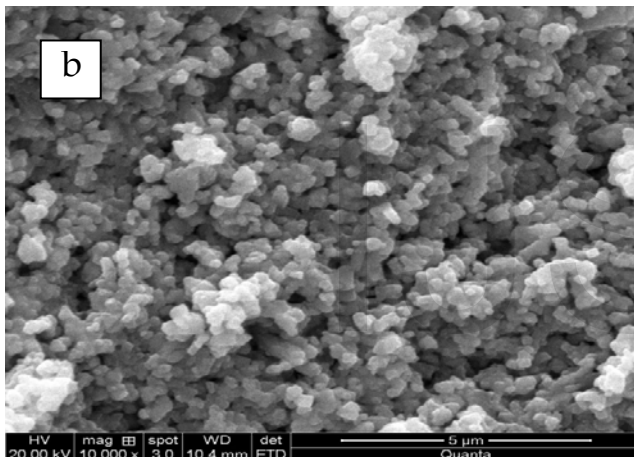
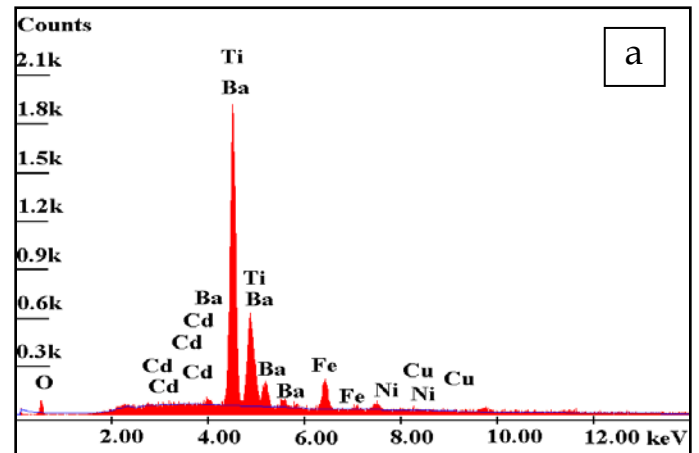
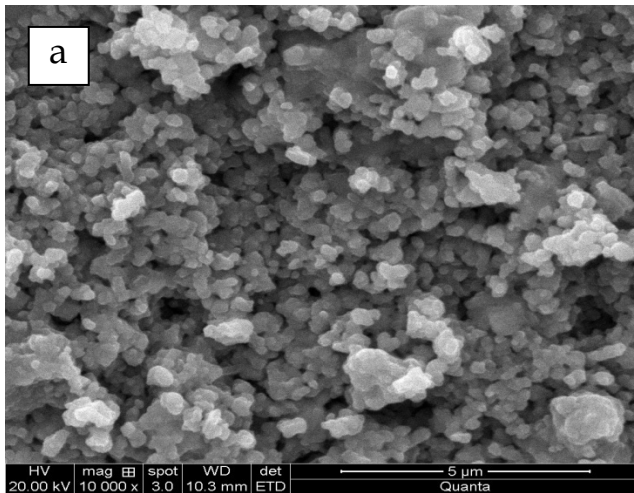


Fig 2. SEM micrographs of (y) $\text{Ni}_{0.75}\text{Cd}_{0.2}\text{Cu}_{0.05}\text{Fe}_2\text{O}_4$ + (1-y) BaTiO_3 ME composites with (a) $y = 0.15$, (b) $y = 0.30$ and (c) $y = 0.45$

Figure 3. EDX spectra of (y) $\text{Ni}_{0.75}\text{Cd}_{0.2}\text{Cu}_{0.05}\text{Fe}_2\text{O}_4$ + (1-y) BaTiO_3 ME composites with (a) $y = 0.15$, (b) $y = 0.30$ and (c) $y = 0.45$

The absence of extra elements other than expected (Ni, Cd, Cu, Fe, O, Ba and Ti) in the EDX spectra reveals the purity of the composites samples and confirms the formation of bi-phases i.e. cubic spinel structure of ferrite phase, tetragonal perovskite structure of ferroelectric phase in the composites.

The absence of third phase in the composites was also confirmed from XRD pattern and SEM micrographs. The estimated weight percentage of the ferrite and ferroelectric phases in the composite are listed in table 2 and are in good agreement with the expected values. In the EDX spectra the peak intensity of Ni, Cd, Cu and Fe (ferrite elements) increases where as the peak intensity of Ba and Ti (ferroelectric elements) decreases with increasing the ferrite content in the composites. A systematic change in intensities of the peaks of ferrite and ferroelectric phases observed in XRD and EDX measurements confirms the effect of percentage composition of ferrite and ferroelectric phases.

3.2. DC electrical resistivity

Electrical resistivity is one of the important properties for the study of ME effect as it gives valuable information about the behavior of free and localized electric charge carriers in the composites. The variation of dc resistivity with temperature is shown in figure 4. In figure 4, it is observed that the resistivity of the composites was constant up to particular temperature and there after it decreases with increasing temperature confirms the semiconducting nature of the samples. Infact, in figure 4 two regions of conductivity we reobserved, first region of conductivity at lower temperature was due to impurities and was attributed to order state of ferroelectric phase and the second region of conductivity at higher temperature was due to polaron hopping and was attributed to disordered paraelectric phase of composites [13]. However, at higher temperatures the impurities present in the system are almost minimized which validated the polaron hopping type of conduction mechanism in composites [14].

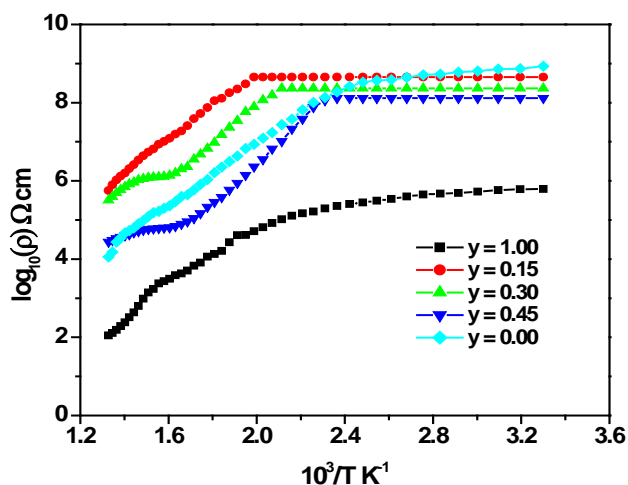


Fig. 4. Variation of dc resistivity with temperature of (y) $\text{Ni}_{0.75}\text{Cd}_{0.2}\text{Cu}_{0.05}\text{Fe}_2\text{O}_4$ + (1-y) BaTiO_3 ME composites.

The decrease in resistivity with increase in temperature was due to the increase in thermally activated drift mobility of charge carriers. The resistivity of the composites was found to decrease with increase of ferrite content this is because resistivity of ferrite phase was small as compared to ferroelectric phase. Also it was observed that the resistivity of the composite samples decreases with increase of average grain size and which was due to the larger average grain size of ferrites compared to ferroelectric phase in the composites. However, electrical conductivity of the composites reduces significantly if the ferrite particles were dispersed throughout the composites to make the chains with ferroelectric particles. The electrical conduction mechanism in the ferrite can be explained on the basis of Verwey and DeBoer [15] mechanism, which involves the exchange of electrons between the ions of the same elements which are randomly distributed over the crystallographic equivalent lattice sites. The exchange of hole between $\text{Ni}^{3+} \leftrightarrow \text{Ni}^{2+} + e^+$, $\text{Cu}^{2+} \leftrightarrow \text{Cu}^{1+} + e^+$, $\text{Cd}^{2+} \leftrightarrow \text{Cd}^{1+} + e^+$ and $\text{Ba}^{3+} \leftrightarrow \text{Ba}^{2+} + e^+$ at low temperature region are responsible for p-type charge carriers and exchange of electron between $\text{Fe}^{2+} \leftrightarrow \text{Fe}^{3+} + e^-$, $\text{Ti}^{3+} \leftrightarrow \text{Ti}^{4+} + e^-$ at high temperature region are responsible for n-type charge carriers and these are responsible for electrical conduction in the composites. Infact, number of such ions depends upon the sintering condition and amount of reduction of Fe^{2+} to Fe^{3+} ions at elevated firing temperature [10].

3.3. Dielectric properties

The variation of dielectric constant with frequency is shown in figure 5. In figure 5 it is observed that in the low frequency region the dielectric constant decreases rapidly up to 1 kHz it may be due to usual dielectric dispersion, where as beyond 1 kHz the dielectric constant gets saturated (high frequency region).

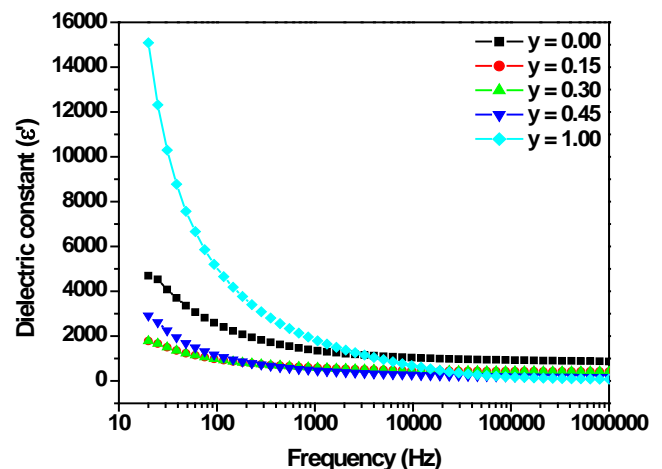


Fig. 5. Variation of dielectric constant with frequency for (y) $\text{Ni}_{0.75}\text{Cd}_{0.2}\text{Cu}_{0.05}\text{Fe}_2\text{O}_4$ + (1-y) BaTiO_3 ME composites.

Infact the decrease of polarization with increase of frequency was observed for almost all composite samples. In the present composite dispersion was due to Maxwell-Wagner [16, 17]

type of interfacial polarization and are in agreement with Koop's [18] phenomenological theory. The invariance of dielectric constant with applied electric field beyond 1 kHz was due to the inability of electric dipoles to follow the alternating field. The maximum value of dielectric constant at low frequency was due to the availability of space charge polarization at the grain boundaries [19]. As the grain size increases the grain boundary area and porosity decreases. The higher value of dielectric constant at low frequency can be explained on the basis of space charge polarization and was due to heterogeneity of dielectric structure; however, heterogeneities are due to grain size and porosity [20]. In these composites at $y = 1.0$ the availability of space charge polarization is maximum at the grain boundaries and hence the dielectric constant is maximum at $y = 1.0$ and minimum at $y = 0.15$. The maximum grain size and minimum grain boundary area at $y = 1.0$, results in the increase of mean free path of electron and hence the dielectric constant becomes maximum at $y = 1.0$. At low frequency region the dielectric constant increases with increase of the ferrite content in the composites, this is because the dielectric constant of ferrite is more compared to ferroelectric phase.

The dielectric loss factor $\tan\delta$ is the energy loss within the material, which is proportional to the imaginary part of the dielectric constant (ϵ''). The dielectric loss was developed when the polarization lags behind the applied ac field and is due to the impurities and imperfections in the crystal lattice. Figure 6 shows the variation of dielectric loss tangent with frequency.

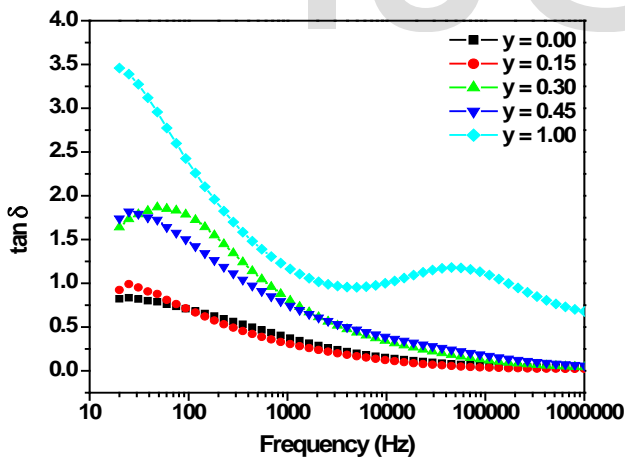


Fig. 6. Variation of dielectric loss tangent with frequency for (y) $\text{Ni}_{0.75}\text{Cd}_{0.2}\text{Cu}_{0.05}\text{Fe}_2\text{O}_4 + (1-y)\text{BaTiO}_3$ ME composites.

In figure 6 we observed abnormal behaviors of the composites as the ferrite content increases. The abnormal behavior may be caused by the collective behavior of two species of charge carriers (p and n) due to the polarization in accordance with Rezluscu and Rezluscu [21]. The local displacement of p-type charge carriers takes part in the polarization in a direction opposite to the n-type of charge carriers in an external electric field. At low frequencies, the contribution of the mobility of

the p-type charge to the polarization decreases more rapidly. The shifting of the position of the peak may be caused by dielectric loss associated with the p-type charge carriers in the composites. The appearance of a peak in dielectric loss factor with frequency curves can be interpreted in terms of correlation between the conduction mechanism and the dielectric behavior in the composites. The peak was appeared when the hopping frequency of electron between $\text{Fe}^{2+}/\text{Fe}^{3+}$ and $\text{Ti}^{3+}/\text{Ti}^{4+}$ is in resonance with the frequency of applied electric field during this mechanism maximum electric energy is transferred to the electrons and the loss shoots up at resonance and also to the domain wall resonance (i.e. grain-grain boundary contribution) [22]. The shift of peak towards higher frequencies with increasing ferrite content suggest smaller relaxation time for composites with $\text{Fe}^{2+}/\text{Fe}^{3+}$ and $\text{Ti}^{3+}/\text{Ti}^{4+}$ ions pairs. The maximum dielectric loss tangent was due to the period of relaxation process similar to that of the period of applied field. If the relaxation time is more as compared to the period of the applied field then the dielectric loss should be small and vice-versa.

Figure 7 shows the variations of $\log(\sigma_{ac}-\sigma_{dc})$ with $\log\omega^2$. The plot shows the linear increase in a.c conductivity with increasing frequency.

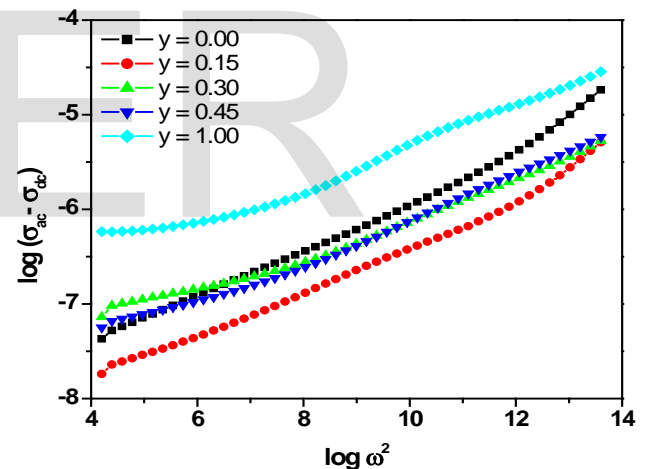


Fig. 7. Variation of ac conductivity with frequency for (y) $\text{Ni}_{0.75}\text{Cd}_{0.2}\text{Cu}_{0.05}\text{Fe}_2\text{O}_4 + (1-y)\text{BaTiO}_3$ ME composites.

In case of the disordered solids the AC conductivity is directly proportional to the frequency and the electrical conduction mechanism is due to electron and polaron hopping models as discussed by Austin and Mott [23] and Appel et.al. [24]. Two polaron models i.e. small polaron and large polaron models were used to explain the conduction mechanism in the composites. The linear increase in conductivity with increasing frequency is attributed to small polaron while the decrease in conductivity with increasing frequency is attributed to large polaron [25]. According to Alder and Feinleib [26] the increase in conductivity with increasing frequency is due to small polarons and is given by the relation.

$$\sigma_{ac} - \sigma_{dc} = \frac{\omega^2 \tau^2}{1 - \omega^2 \tau^2} \quad (8)$$

Where, ω is the angular frequency, τ is the relaxation time (10^{-10} S) for all ceramics (if $\omega^2 \tau^2 < 1$). The linear increase of AC conductivity with frequency indicates small polaron type of conduction mechanism in the composites but a slight decrease in conductivity at certain frequency is attributed to mixed polaron (i.e. small and large) conduction mechanism in the composites [27]. Hence the present composites show small polaron hopping type of conduction mechanism.

3.4. Multiferroic properties

3.4.a. Ferromagnetic hysteresis studies

The magnetic hysteresis loops of the composites as a function of ferrite content is shown in figure 8. The magnetic hysteresis loops at room temperature indicates the presence of an ordered magnetic structure in the mixed cubic spinel and tetragonal perovskite systems in the composites.

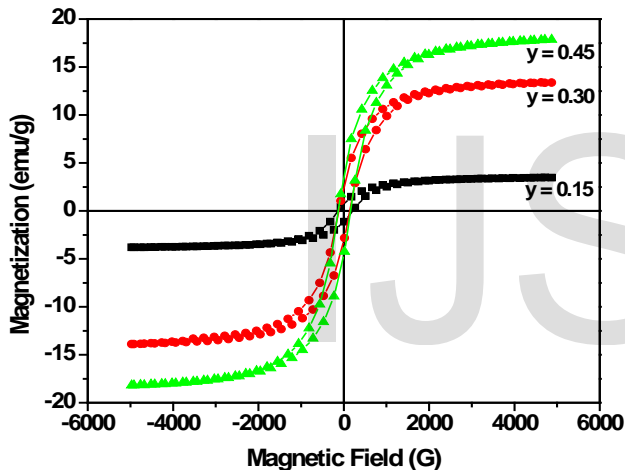


Fig. 8. Magnetic hysteresis loop of (y) $\text{Ni}_{0.75}\text{Cd}_{0.2}\text{Cu}_{0.05}\text{Fe}_2\text{O}_4$ + (1-y) BaTiO_3 ME composites.

As the ferrite content decreases the magnetic hysteresis loop shifts towards the field axis in the composites. The estimated saturation magnetization and magnetic moment are listed in table 2. The saturation magnetization, remnant magnetization and magnetic moment of the composite gradually decrease with increase of ferroelectric content. Thus ferroelectric phase decreases the contribution of magnetization of the ferrite phase in the composites [28]. The observed and theoretical values of saturation magnetization and magnetic moment of the composites with different ferrite concentration (Fig. 9) shows similar behavior as reported for Ni-Co ferrite / BPZT [12] and Ni-Co-Cu ferrite / BaTiO_3 composites [29]. The magnetic parameter of the composites increases with increasing the ferrite content and it was due to the contribution of individual ferrite grains. The decrease of average grain size and porosity with increase of the ferrite content affects the magnetization. The saturation magnetization and magnetic moment

decreases with increasing the ferroelectric phase as the non-magnetic ferroelectric material acts as pores in the presence of magnetic field, which breaks the magnetic circuit between the grains and results in the decrease of magnetic properties [30].

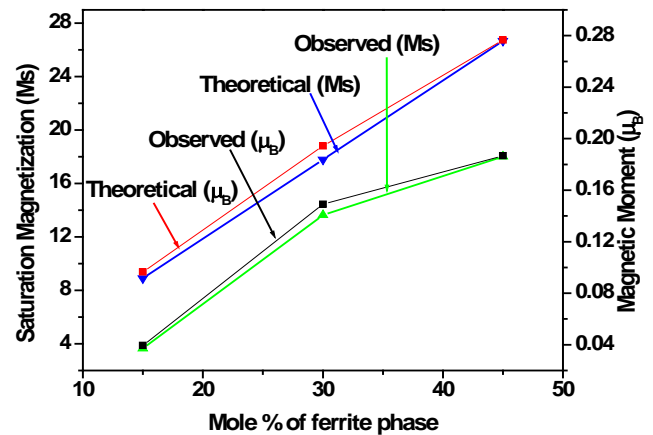


Fig. 9. Variation of saturation magnetization and magnetic moment of (y) $\text{Ni}_{0.75}\text{Cd}_{0.2}\text{Cu}_{0.05}\text{Fe}_2\text{O}_4$ + (1-y) BaTiO_3 composites with ferrite content

The temperature dependent magnetization of the composites with different ferrite concentration is shown in figure 10.

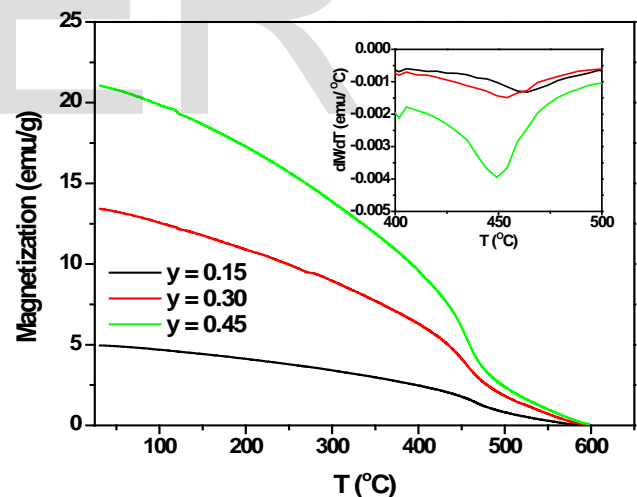


Fig. 10. Variation of magnetization with temperature for (y) $\text{Ni}_{0.75}\text{Cd}_{0.2}\text{Cu}_{0.05}\text{Fe}_2\text{O}_4$ + (1-y) BaTiO_3 ME composites.

The magnetization of the composites decreases with increase of the temperature up to certain temperature thereafter there is a change in the slope of magnetization; this particular temperature is called as magnetic transition temperature. The magnetic transition temperature of the composites can be estimated from the minimum position of the dM/dT with temperature plot as shown in the inset of figure 10. The estimated magnetic transition temperatures of the composites are listed in table 2. The estimated magnetic transition temperature of

the composites decreases with increase of the ferrite content and it was due to the weakening of the A-B exchange interaction. Infact, weakening was due to the increase of A and B sizes and was confirmed by the increase of lattice parameter of ferrite phase in the composites.

3.4.b. Ferroelectric hysteresis studies

The ferroelectric hysteresis loops of the composites measured at room temperature at two different frequencies are shown in figure 11 (a-c).

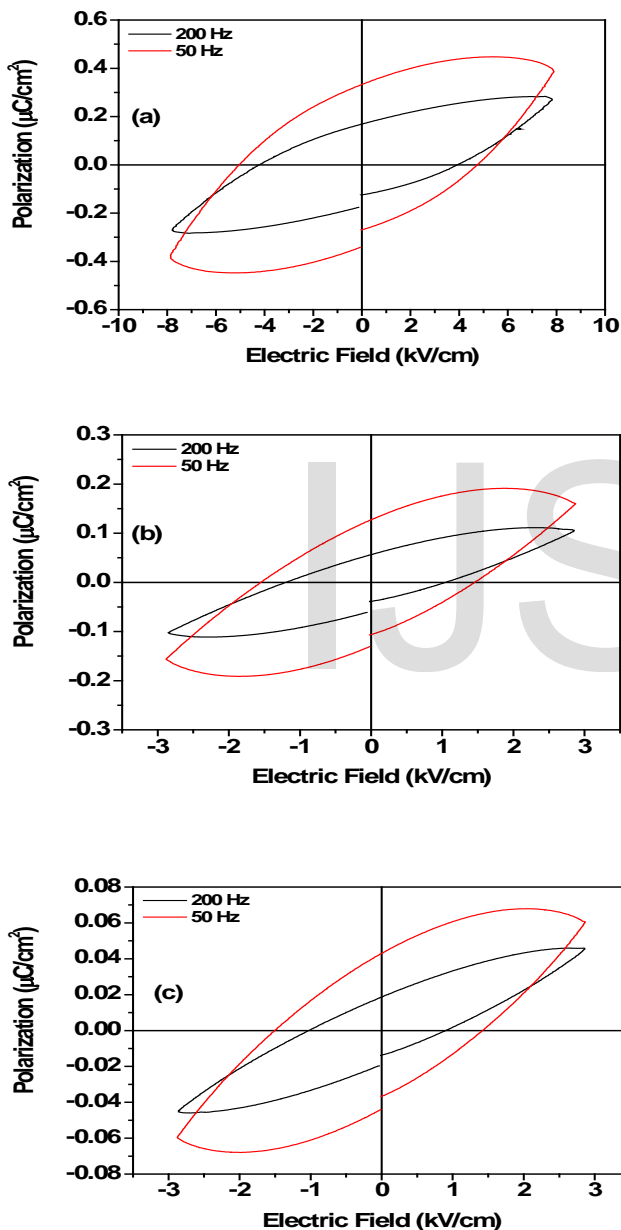


Fig. 11. Ferroelectric hysteresis loop of (y) $\text{Ni}_{0.75}\text{Cd}_{0.2}\text{Cu}_{0.05}\text{Fe}_2\text{O}_4 + (1-y)\text{BaTiO}_3$ ME composites with y = 0.15, (b) y = 0.30 and (c) y = 0.45.

It shows similar behavior as that of the ferromagnetic material but polarization values decreases with increase of ferrite content. At high frequency region we notice the decrease of polarization with increase of frequency and were assigned to the

capacitance effect [31, 32]. The leakage of current in the composites was due to the decrease of electric dipole interaction and decrease of polarization contribution of the ferroelectric phase with increasing the non-electric (ferrite) phase in the composites. The ferrite phase mixed with ferroelectric phase acts as pores in the presence of applied electric field and breaks the electric circuit, resulting in the decrease of ferroelectric parameters like saturation polarization and remnant polarization. The saturation polarization and remnant polarization of the composites increase with ferroelectric content (table 2) this is because the individual ferroelectric grains acts as centre of polarization. The saturation polarizations of the composites are the vector sum of all these individual contributions.

3.4.c. Magnetoelectric effect

The variations of static magnetoelectric voltage coefficient with applied dc magnetic field of these composites are in figure 12. From the figure we notice that the magnetoelectric voltage coefficient gradually increases initially and attains maximum value then thereafter decreases with applied dc magnetic field. The initial increase of magnetoelectric voltage coefficient was attributed to the enhancement in elastic interaction and was confirmed by the hysteresis measurements. The maximum value of magnetoelectric voltage coefficient indicates the saturation value of magnetosrictive phase. The decrease of magnetoelectric voltage coefficient after reaching a maximum value with increasing the magnetic field was due to the induced strain due to the magnetostrictive phase. Infact, the electric field produced in the ferroelectric phase during magnetic poling process decreases the magnetoelectric voltage coefficient with increasing the applied dc magnetic field [32].

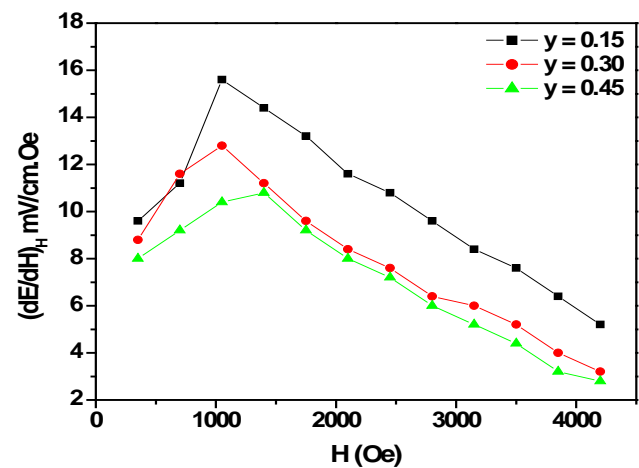


Fig. 12. The variation of static magnetoelectric voltage coefficient with dc magnetic field at room temperature for (y) $\text{Ni}_{0.75}\text{Cd}_{0.2}\text{Cu}_{0.05}\text{Fe}_2\text{O}_4 + (1-y)\text{BaTiO}_3$ ME composites

The ME response in bulk ME composites are depending on the material properties of the magnetostrictive phase i.e. ferrite phase. The origin of ME output in these ME composites are due to the magnetic – mechanical – electric interaction, as it is

depends on the magnetic properties of the magnetostrictive phase. Thus ME output originates due to the electric coupling between ferrite-ferroelectric grains. Uniform distribution of piezomagnetic grains into the piezoelectric matrix is one of the essential factors to obtain high ME response in the composites. The decrease of magnetoelectric voltage coefficient with increasing ferrite content in the composites was due to the increase of magnetostrictively induced strain of the composites, where the resistivity of the composites decreases, leakage current reduces due to the connection between the ferrite grains and the interfacial effect. The maximum magnetoelectric voltage coefficient of 15.6 mV / cmOe was observed for $y = 0.15$ and it was due to the correlation between the grain distribution in ferrite and ferroelectric phases in the composites.

3.4.d. Effect of grain size on magnetoelectric effect

The variations of static magnetoelectric voltage coefficient with ferrite content in the composites are shown in the figure 13. Figure shows the decreases of static magnetoelectric voltage coefficient with increasing the ferrite content in the composites. The static magnetoelectric voltage coefficient was also decreases with increase of average grain size as the average grain size increases with mole % of ferrite phase. However, the larger average grain sizes are less effective in inducing piezomagnetic and piezoelectric coefficient rather than the smaller ones [12]. Thus magnetoelectric voltage coefficient depends on mole % of constituent phases in the composites. Figure 13 clearly shows that the maximum magnetoelectric voltage coefficient for $y = 0.15$ and minimum for $y = 0.45$, as the average grain size is minimum for $y = 0.15$ and maximum for $y = 0.45$ mole % of ferrite phase in the composites. Thus smaller grain sizes of the samples play crucial role for getting the maximum magnetoelectric (ME) output in the composites.

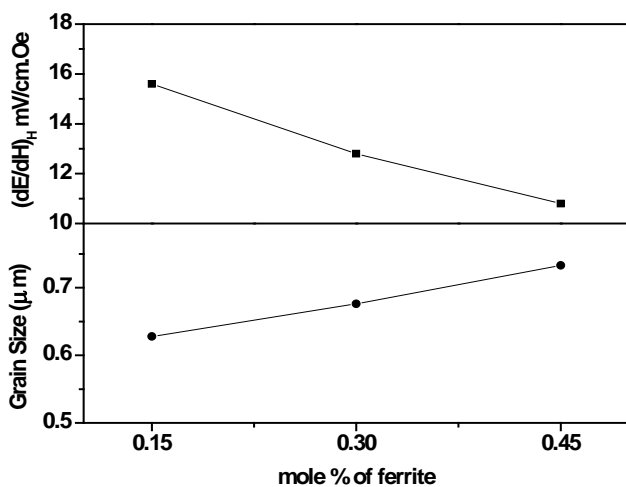


Fig. 13. Variation of static magnetoelectric voltage coefficient and average grain size with mole % of ferrite for $(y) \text{Ni}_{0.75}\text{Cd}_{0.2}\text{Cu}_{0.05}\text{Fe}_2\text{O}_4 + (1-y) \text{BaTiO}_3$ ME composites

3.4.e. Effect of resistivity on magnetoelectric effect

The variation of magnetoelectric voltage coefficient and dc

resistivity with ferrite content is shown in figure 14. In the figure it is to be noted that magnetoelectric voltage coefficient was found to be highest for high resistivity composite samples as it depends on mole % of constituent phases in the composites. The magnetoelectric voltage coefficient was found to be maximum for 15 mole % and minimum for 45 mole % of ferrite phase in the composites. This indicates that high resistivity samples induces high magnetoelectric voltage coefficient and low resistivity samples induces low magnetoelectric voltage coefficient; similar behavior was reported by Patil et.al. [33].

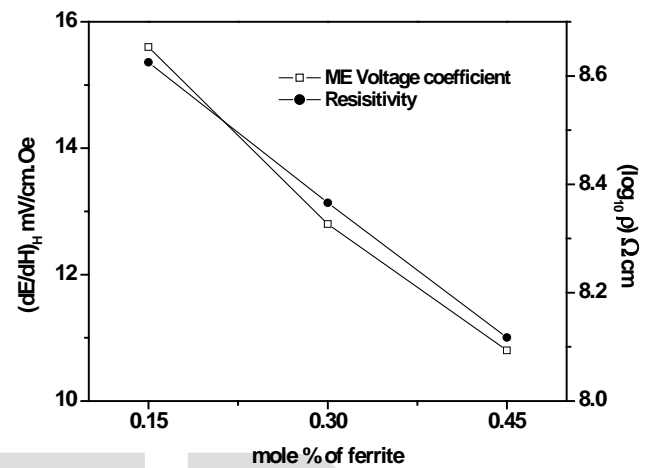


Fig. 14. Variation of ME voltage coefficient and dc resistivity with mole % of ferrite content for $(y) \text{Ni}_{0.75}\text{Cd}_{0.2}\text{Cu}_{0.05}\text{Fe}_2\text{O}_4 + (1-y) \text{BaTiO}_3$ ME composites

The composites with high ferrite phase cannot be poled at a high electric voltage as it has low resistance compared to ferroelectric phase and therefore one cannot get high piezoelectric effect due to the leakage of charges developed in the ferroelectric grains surrounded by ferrite grains with low resistance path. Thus the leakage of charges reduces the magnetoelectric effect in the composites.

TABLE-1 (a): The Lattice Parameter, Porosity of Composites and its Constituent Phases

(y)	Lattice parameters of phases (Å)				Porosity (%)
	Ferrite 'a'	Ferroelectric			
		'a'	'c'	'c/a'	
0.00	-	3.999	4.000	1.0002	23.22
0.15	8.326	3.999	4.000	1.0002	20.39
0.30	8.362	3.998	3.999	1.0002	19.98
0.45	8.387	3.999	4.000	1.0002	14.98
1.00	8.402	-	-	-	13.11

TABLE- 1 (b): Average Grain Size, % of Composition of Composites and its Constituent Phases

(y)	Average grain size (μm)	Percentage of composition (%)			
		Ferrite		Ferroelectric	
		Expected	EDX	Expected	EDX
0.00	0.799	-	-	100	100
0.15	0.628	15	13.72	85	86.27
0.30	0.676	30	28.74	70	71.25
0.45	0.733	45	43.57	55	56.42
1.00	1.759	100	100	-	-

TABLE- 2: Saturation Magnetization (M_s), Magnetic Moment (μ_B), Saturation Polarization (P_s), Remnant Polarization (P_r) and Magnetic Transition Temperature (T_c).

(y)	M_s (emu/gm)	μ_B	P_s P_r ($\mu\text{C}/\text{cm}^2$) at 50 Hz		T_c $^\circ\text{C}$				
			0.00	-		-	0.574	0.241	-
			0.15	03.64		0.039	0.385	0.333	463
0.30	13.63	0.149	0.160	0.127	454				
0.45	18.02	0.186	0.060	0.043	449				
1.00	59.30	0.546	-	-	-				

4. Conclusion

The ME composites of our interest was synthesized by standard double sintering ceramic method. The XRD pattern obtained for all the composites reveals the confirmation of biphased i.e. cubic spinel structure of ferrite phase and tetragonal perovskite structure of ferroelectric phase in the composites. The average grain size was found to increase with ferrite content in the composites. The non-appearance of extra elements other than Ni, Cd, Cu, Fe, O, Ba and Ti in the EDX spectra; reveals purity of the composites and was also confirmed from XRD patterns, SEM micrographs and EDX spectra's of the composites. All the composites exhibits semiconducting nature as the temperature increases the dc resistivity of the composites decreases. The variation of dielectric constant and dielectric loss tangent with frequency shows the usual dielectric dispersion behavior in the low frequency region and almost constant at high frequency region was due to Maxwell-Wagner type of interfacial polarization. The linear variation of a.c conductivity with frequency shows small polaron type of conduction mechanism in the composites. The ferromagnetic and ferroelectric hysteresis behaviors of all the composites were studied with ferrite content. The magnetic parameters of the composites i.e. saturation magnetization and magnetic moments are found to increase while magnetic transition temperature are found to decrease with increasing the ferrite content. The saturation and remnant polarization of the com-

posites are found to decrease with increasing the frequency as well as the ferrite content. The maximum ME conversion factor of 15.6 mV/cmOe was observed for the composites with 15 % of ferrite and 85 % ferroelectric phases. And from the study of effect of grain size as well as resistivity on the ME effect it was observed maximum ME voltage coefficient for high resistivity and small average grain size of the composite samples.

Acknowledgement

One of the authors (LRN) is grateful to UGC, New Delhi, for sanctioning the major research project. The author (PBB) thanks to CSIR, New Delhi, for awarding Senior Research Fellow (SRF). Authors are thankful to Dr. V. R. Reddy, UGC-DAE, CSR, Indore (MP), for providing ferroelectric loop tracer experimental facilities

References

- [1] C.A.F. Vaz, J. Hoffman, C.H. Ahn, R. Ramesh, *Adv. Mater.* 22 (2010) 2900-2918.
- [2] C.W. Nan, M. Bichurin, S.X. Dong, D. Viehland, G. Srinivasan, *J. Appl. Phys.* 103 (2008) 031101.
- [3] M. Jing, H. Jiamian, L. Zheng, C.W. Nan, *Adv. Mater.* 23 (2011) 1062-1087.
- [4] W. Eerenstein, N.D. Mathur, J.F. Scott, *Nature.* 442/17 (2006) 759.
- [5] R. Ramesh, N.A. Spaldin, *Nature Mater.* 6 (2007) 21.
- [6] J. V. Suchtelene, *Philips. Res. Rep.* 27 (1972) 28.
- [7] G.A. Smolenskii, I.E. Chupis, *Sov. Phys. Usp.* 25 (1982) 475.
- [8] C.W. Nan, D.R. Clarke, *J. Am. Ceram. Soc.* 80 (1997) 1333.
- [9] J. Ryu, S. Priya, K. Uchino, H.E. Kim, *J. Electroceram.* 8 (2002) 107.
- [10] P. B. Belavi, G. N. Chavan, L. R. Naik, R. K. Kotnala, *Inter. J. Nanosci.* Vol. 11, No. 3 (2012) 1240007 (5pp).
- [11] A. Cottrell, *An Introduction to Metallurgy*, Edward Arnold Publishing Ltd, London, 1967.
- [12] B. K. Bammannavar, L. R. Naik, B. K. Chougule, *J. Appl. Phys.* 104 (2008) 064123.
- [13] R. P. Mahajan, K. K. Patankar, A. N. Patil, S. C. Choudhary, A. K. Ghatage, S. A. Patil, *J. Eng. Mater. Sci.* 7 (2000) 203.
- [14] R. N. P. Choudhary, S. R. Shannigrahi, A. K. Singh, *Bull. Mater. Sci.* 22 (6) (1999) 75.
- [15] E. J. W. Verwey, F. De. Boer, J. H. Vsanten, *J. Chem. Phys.* 161 (1948), p. 1091.
- [16] J. C. Maxwell, *Electricity and Magnetism*, Vol. 2 Oxford, University Press, New York, 1973, p. 828.
- [17] K. W. Wagner, *Am. J. Phys.* 40 (1933) 817.
- [18] C. G. Koops, *Phy. Rev.* 83 (1951)121.
- [19] L. T. Rabinkin, Z. I. Novikova, *Acad Nauk, USSR Minsk*, 1960, p. 146.
- [20] Y. B. Kamble, S. S. Chougule, B. K. Chougule, *J. Alloys. Comp.* 476 (2009) 733.
- [21] N. Rezluscu, E. Rezluscu, *Phys. State. Solid. (a)* 23 (1973) 575.
- [22] D. Ravinder, K. Vijayakumar, *Bull. Mater. Sci.* 24 (5) (2001) 505.
- [23] I. G. Austin, N. F. Mott, *Adv. Phys.* 18 (1996) 411.

- [24] J. Appel, F. Seitz, D. Thumbull, E. Ehrenreich, Soild. State. Phys. 21 (1968) 193.
- [25] K. K. Patnakar, S. S. Joshi, B. K. Chougule, Phys. Lett. A 346 (2005) 337.
- [26] D. Alder, J. Feinleib, Phy. Rev. B 2 (1970) 3112.
- [27] J. B. Goodenough, Prog. Solid. Stat. Chem. 5 (1971) 145.
- [28] H. Su, H. Zhang, X. Tang, Y. Jing, Z. Zhong, J. Magn. Mater. 321 (2009) 2763.
- [29] R. S. Devan, B. K. Chougule, J. Appl. Phys. 101 (2007) 014109.
- [30] R. C. Kamble, P. A. Shaikh, C. H. Bhosale, K. Y. Rajpure, Y. D. Kolekar, J. Alloys. Compd. 489 (2010) 310.
- [31] W. Chen, Z. H. Wang, W. Zhu, U. K. Tan, J. Phys. D; Appl. Phys. 42 (2009) 075421.
- [32] N. Cai, J. Zahi, C. W. Nan, Y. Lin, Z. Shi, Phy. Rev. B 68 (2003) 224103.
- [33] D. R. Patil, B.K. Chougule, J. Alloys. Comp. 470(1-2) (2009)

IJSER